An experimental survey in the wake of a simulated tidal current turbine

X Sun BSc, MSc, PhD; IG Bryden BSc PhD; H Jeffrey BEng, MBA, Institute for Energy Systems, Joint Research Institute for Energy, School of Engineering and Electronics, The University of Edinburgh, Scotland
D Forehand BSc, MSc, PhD, PGCE, Department of Mechanical Engineering, The University of Glasgow, Scotland

This paper presents two experimental test programmes, conducted in a water flow channel and a tow tank respectively, and devised to investigate the wake behind a simulated horizontal axis tidal current turbine. Both sets of experimental results have identified the wake as having a Gaussian-like shape and the wake deficit recovering gradually with distance downstream. Also, although it is not directly representative of real operating conditions, the appropriateness of a towing tank for the model tidal current turbine testing has been supported, by having obtained compatible force and wake profiles in the two test programmes

AUTHORS' BIOGRAPHIES

Xiaojing Sun recently completed her PhD in the Institute of Energy Systems at the University of Edinburgh where she worked in the SuperGen Marine Research Consortium. Prior to starting her PhD, she gained her BSc (China, 1999) and MSc (UK, 2003) degrees in Civil Engineering.

Professor Ian G Bryden holds the Chair of Renewable Energy in the University of Edinburgh, having been involved in marine renewable energy research since 1980. He is a Fellow of IMarEST, The Institution of Mechanical Engineers and the Institute of Physics.

Henry Jeffrey is a research fellow at the University of Edinburgh. He has extensive marine energy experience in the private and public sectors and was part of the project team that installed the word's first commercial grid connected wave energy device.

David Forehand obtained his PhD in Computational Fluid Dynamics in 1998 and has worked as a researcher in the fields of Nonlinear Engineering Dynamics at the University of Glasgow and Tidal Power at The Robert Gordon University.

INTRODUCTION

There are substantial tidal current energy resources in the UK because of its natural geographic features. A comprehensive assessment of tidal current resource in the UK was carried out as early as 1993 by the UK Department of Trade and Industry's Energy Technology Support Unit (ETSU). Its report identified the most promising tidal sites for exploitation and estimated that, if all potential sites were developed, 10% of the UK electrical supply could be generated using tidal currents.[1] Publications by the Carbon Trust[2] and the Scottish Executive[3] have supported tidal currents as potential strategically significant sources of energy. In addition, a recent report[4] by the Sustainable Development Commission (SDC), although primarily relating to tidal barrage development, also included a significant section relating to tidal current development and is indicative of continuing national interest in the field.

Hence, research into the precise estimation of tidal current energy resources, as well as the development of energy converter prototypes is being widely conducted. One recent important development is that a full-scale 1.2MW, twin rotor tidal current device has been successfully

NOMENCLATURE

A = area of perforated disk (m^2)
C_t = rotor thrust coefficient
d = perforated disk diameter (m)
g = gravitational acceleration (m/s^2)
h = submerged water depth of the test perforated disk (m)
M = turbulence-generating grid mesh size (m)
T = thrust force (N)
U_0 = free stream velocity (m/s)
U_w = wake velocity (m/s)
U_c = velocity on wake centerline (m/s)
ρ = water density (kg/m^3)

designed and installed in Strangford Lough in Northern Ireland by Marine Current Turbines Ltd. Similarly, a tidal current device has been installed in the European Marine Energy Centre (EMEC) by Open Hydro Ltd and has recently begun supplying electricity to the grid. At present, the cost of generation from tidal currents is still considered too high for economic development and further reductions in the generation costs will depend on large-scale exploitation and lower deployment costs to make the tidal current energy market competitive. As individual devices are unlikely to exceed rated capacities of 2MW, energy converters will need to operate together at a tidal site, forming a 'farm'.

The wake created behind every tidal energy turbine in the process of energy extraction is characterised by reduced water speeds and high turbulence levels. Within a tidal 'farm', some devices could work in the wake of the upstream devices and consequently produce less energy due to their reduced inflow. In addition, the higher levels of turbulence introduced by the wake can increase the fatigue load on the downstream devices and could minimise their lifetime.[5] In order to maximise the overall energy output from a tidal 'farm', the wake effect is an essential factor in determining the optimal spacing between tidal current turbines arranged in rows. Tidal current turbines work in a highly restricted environment[6] and could be installed in close proximity to the free surface and seabed. The parameters that govern the wake structure and its recovery are likely to be different for tidal current turbines and wind turbines, despite their superficial similarity. These parameters have already been explicitly discussed.[7]

This paper presents two experiments that were designed and performed to investigate flow characteristics of wakes downstream of a tidal current turbine. A water flow channel and a towing tank were intentionally chosen as the experimental facilities, with the purpose of identifying the influence of different flow conditions on the tidal current model testing.

EXPERIMENT SET-UP

When a horizontal axis turbine rotates with a high tip speed ratio, the turbine will start to perform as a disk[8,9] and, moreover, the wake behind it is quite similar to that behind a stationary 'disk-like' body.[10-11] In addition, the thrust force acting upon the turbine, the force generated by the pressure difference across the rotor due to energy extraction, is the most critical factor in determining the nature of the downstream wake and needs to be effectively simulated in the experiment. Therefore, perforated disks are widely accepted as a representative, yet simple, horizontal axis turbine model and have been utilised for wake study. A series of thrust forces can be determined by varying the porosity of the disk.

Aluminum disks of 5mm thick and 250mm diameter were constructed and tested as simulated tidal current turbines in experiments. Circular holes were drilled in the disk to allow the water through and were distributed as uniformly as possible, with a range of porosities (the ratio of the total area of holes to the disk area) from 14% to 50%.

Thrust force was measured by an 'S' beam load cell. The active end of the load cell was tightly attached to a 19mm × 19mm aluminum strut using a bolt and was set firmly on a test support frame. The other end of the strut held the perforated disk, which was suspended from the load cell. The force produced by water moving through the test disk caused deformation of the load cell through the strut in a cantilever manner and thus the force acting upon the disk could be measured. The test rig is shown in Fig 1. Before each experiment started, the load cell was re-calibrated.

In-house fabricated pitot probes were adopted for the mean velocity measurements in the wake. They have the conventional configuration of a pitot tube and 20mm diameter nylon rod bars were used for the main body. A 6mm

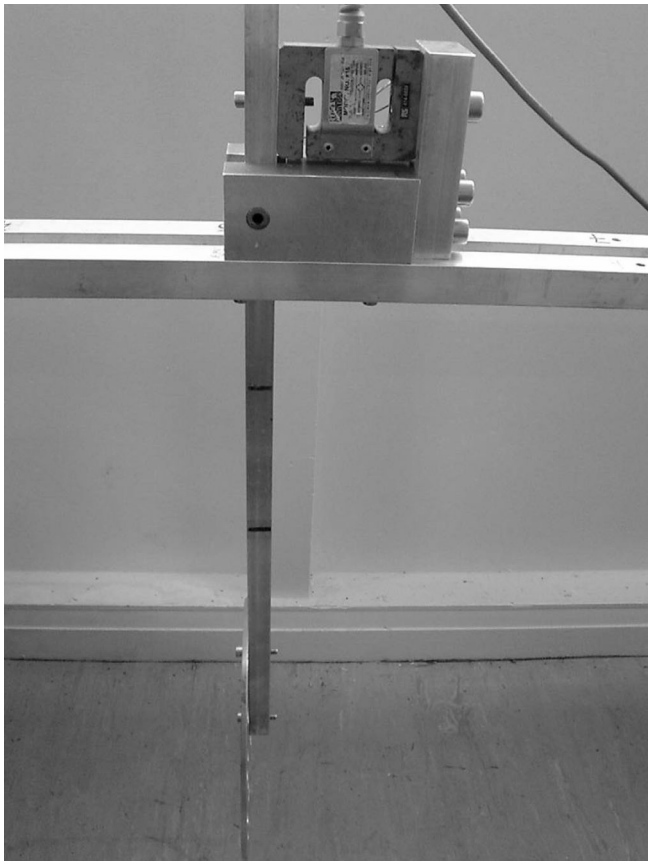

Fig 1: The test rig for force measurement

diameter stagnation hole was drilled at the front of each rod bar and three 6mm diameter static holes were drilled 125mm downstream from the stagnation hole on three sides of the pitot probe. A miniature piezoresistive pressure transducer, which has an operating range from 0 to 0.5 psi, was enclosed in the rectangular cavity cut in the pitot probe, and the cavity was finally sealed with a transparent silicone elastomeric compound, which can effectively protect and insulate the transducer from the water.

The two pressure inlet ports of the pressure transducer were connected respectively to the plastic tubing: one from the stagnation hole and the other from static holes, in order to 'sense' the differential pressure. This design, by containing the differential pressure transducer inside the body of the pitot probe, can significantly minimise the length of the tubing between measured holes and transducer and thus give the transducer a fast response time. Five completed pitot probes were assembled and mounted on a pedestal to form a pitot probe rake. The centre-to-centre spacing between pitot probes was 100mm in order to minimise interference. The pitot tube rake could also be rotated 90 degrees around its vertical support and, therefore, the velocity profiles in both the vertical and horizontal planes across the wake could be measured. Each pitot probe was calibrated and its measurement accuracy determined to be within $\pm$ 4%, by comparing the output of the pitot probe with the precisely predefined speeds of the towing carriage in a towing tank. The pitot probe and pitot probe rake is presented in Fig 2.

Fig 2: The pitot probe rake

EXPERIMENTS IN A WATER FLOW CHANNEL

The test site selected was at Quoich Power Station on the river Garry near Invergarry and is a concrete lined channel with a width of 3m and a length of 3.3m. A horizontally configured bar screen formed the bottom of channel, which could be manually lifted above the water surface by a hoist. The water depth inside the channel could reach 0.95m. The Reynolds number based on the mean flow speed and the hydraulic radius of the channel had an order of 10^5 and thus was much larger than 2000, the value of the Reynolds number, at which transition to turbulence in an open channel occurs. Therefore, the water inside the channel was judged to be a fully developed turbulent flow, as shown in Fig 3.

Before the experiment started, a 1m high test support frame, which was fabricated to support the test disk and the measurement instrumentation, was fixed on the screen bar in the middle of the channel. The front of the frame was approximately 0.5m from the inlet region of channel. An 8-channel datascan system was employed to convert the analog input signal from the load cell and pressure transducers to digital values, which could be logged in a computer, which was connected to the datascan through an RS232 cable. The sampling rate was 1Hz and data were recorded for 60 seconds at each measurement position. These tests were designed to generate time averaged records, for which the sampling rate was deemed adequate. The instrumentation noise in the measurements was neglected as it was considerably less than the flow induced fluctuations in output, which for both the moving water tests and the tow tank tests represented an RMS of approximately 10% of the time averaged results.

Two 12V batteries wired in series powered the datascan and provided excitation voltage for the load cell and the transducers. Batteries and the datascan were put separately in waterproof boxes and mounted on the test support frame. It should be appreciated that the measurement site was remote from any appreciable laboratory support and this represented a considerable challenge to the experimenters.

The undisturbed free stream velocity at different positions in the channel was measured by the pitot probe rake

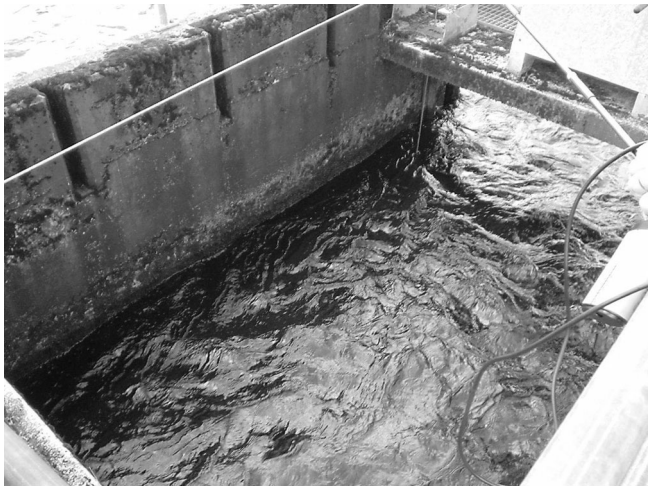

Fig 3: Close up of water within the water flow channel

before the test disk was placed in position. It was found, not too surprisingly, that the water velocities were greatest near the surface and reduced with increasing measurement depth, as displayed in Fig 4(i), which clearly illustrates the mean velocity gradient in an open channel flow. But the velocity profiles in the horizontal plane are nearly constant, which are shown in Fig 4(ii). Velocities measured at the hub height of perforated disk were averaged and used as the mean free stream velocity U_0, which was 0.76 ($\pm$0.03) m/s. Afterwards, the bar screen was lifted above the water to set the load cell and perforated disk on the test support frame and, at the same time, the outputs of load cell and pressure transducers were recorded as their offsets for later force and velocity calculations. Then, the bar screen was lowered into the water until the water depth reached to 0.95m and the submerged depth of test disk h, the distance from the water surface to the centre of perforated disk, was 0.35m (1.4d). The velocity measurements were conducted at 3d, 4d and 6d downstream of the disk respectively and the mean velocity profiles in the vertical and horizontal planes of the wake downstream of the perforated disk were measured. Since the ratio of the perforated disk area to the channel section was 1.7%, which was relatively insignificant, no corrections were made to take account of the influence of blockage effect on the velocity measurements. A schematic diagram of the experimental setup in the water flow channel is shown in Fig 5.

EXPERIMENT IN A TOWING TANK

The second experiment was performed in a towing tank located at the Acre Road Hydrodynamics Laboratory, which is operated jointly by the Universities of Glasgow and Strathclyde. The tank has a total length of 70m, with a rectangular cross section of 4.6m (width) $\times$ 2.4m (depth), as shown in Fig 6.

During the test, the perforated disk and pitot probe rake were attached to a towing rig and pulled through still water at a steady speed to simulate a uniform current. The submerged depth of the test disk h was 0.35m, which was the same as the depth in the water flow channel. Care was taken to ensure that the disk and the pitot probes were perpendicular to the incoming flow so as to obtain symmetric inflow conditions. The blockage ratio in the towing tank was 0.4%, which can be ignored. In order to make a close comparison of these two experiments, turbulence was introduced into the water by means of a turbulence-generating grid. It consisted of an array of 19mm square wooden bars, which were arranged in a checkerboard pattern with a mesh size M of 163mm centre-to-centre spacing. The larger mesh size M was utilised in an attempt to reduce the resistance of the grid to incoming flow. The free stream speed U_0 at the position of perforated disk was 0.8m/s. Therefore, the grid Reynolds number, based on M and U_0 was 1.35×10^5, which was relatively large to ensure a fully developed turbulence initial state downstream of the grid. With consideration of the time needed to complete all the experiments, the wake measurements were only taken 3d and 4d behind the test disk respectively and approximately 15M and 16M downstream from the turbulence-generating grid,

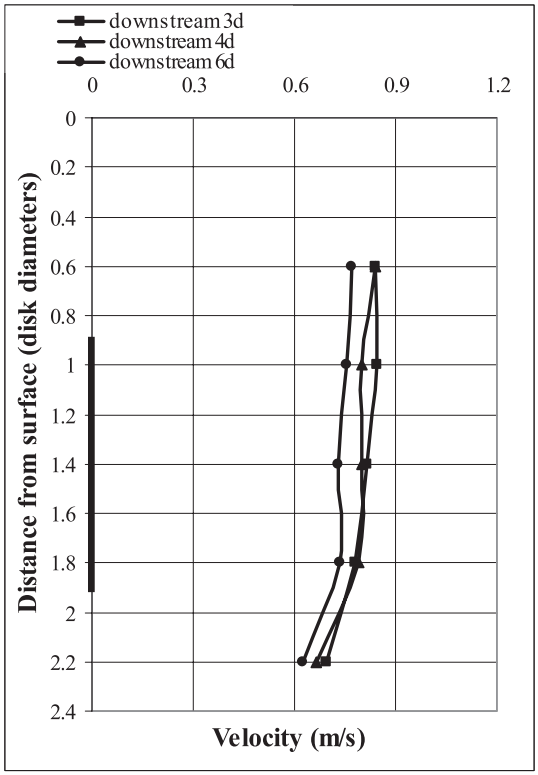

(i)

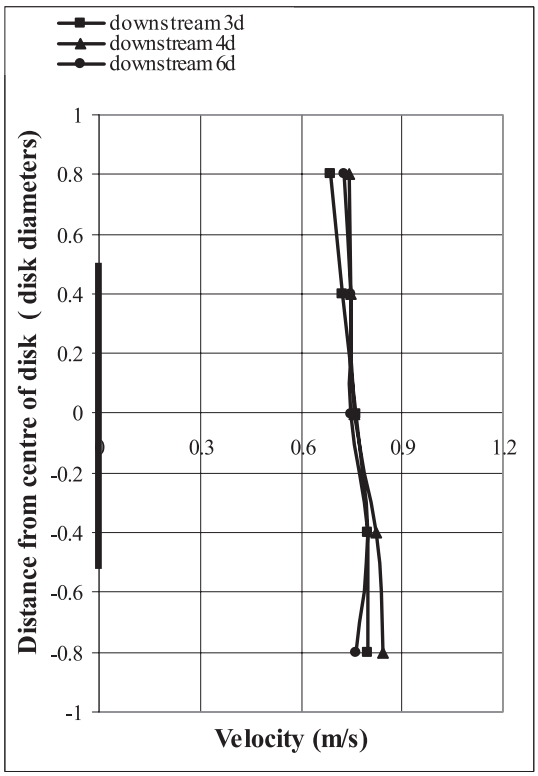

(ii)

Fig 4 (i): The initial velocity profiles in the central vertical plane at 3, 4 and 6 diameters behind the test disk in the water flow channel (the top line along the zero water depth represents the free surface)

Fig 4 (ii): The initial velocity profiles in the central horizontal plane at 3, 4 and 6 diameters behind the test disk in the water flow channel

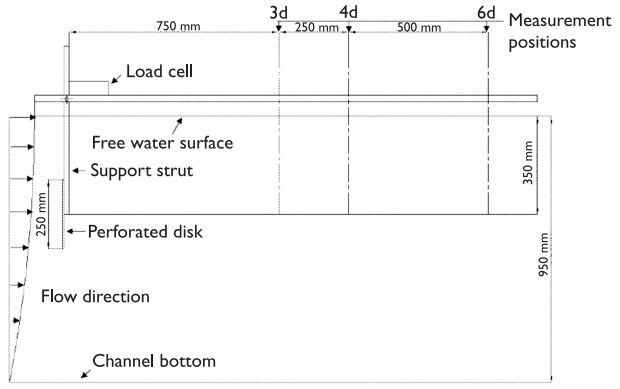

Fig 5: A schematic overview of the experimental setup in the water flow channel

Fig 6: The towing tank

where the grid turbulence was considered to become homogeneous.

Before the perforated disks were tested, the initial velocity profiles behind the turbulence-generating grid were measured, shown in Fig 7(i) & (ii). The overall experimental setup for the measurements with the turbulence-generating grid attached in the towing tank is shown in Fig 8.

RESULTS AND DISCUSSION

Raw data recorded on the computer were processed for the force and wake velocities calculations. Thrust force on the perforated disk was obtained from the calibration curve of the load cell. Fluctuations of the force were observed, which were caused by turbulence in the flow. Averaged force T was converted to thrust force coefficient C_t using equation (1).

$$C_t = \frac{T}{0.5\rho U_0^2 A} \quad (1)$$

The wake velocities U_w were calculated using equation (2), in which the differential pressure Δp was measured by the pitot probe. In both experiments, the outputs from the pressure transducer were collected by the datascanner and were averaged over the period of record. The voltages were then converted into differential pressure using the calibration equation for each pitot probe.

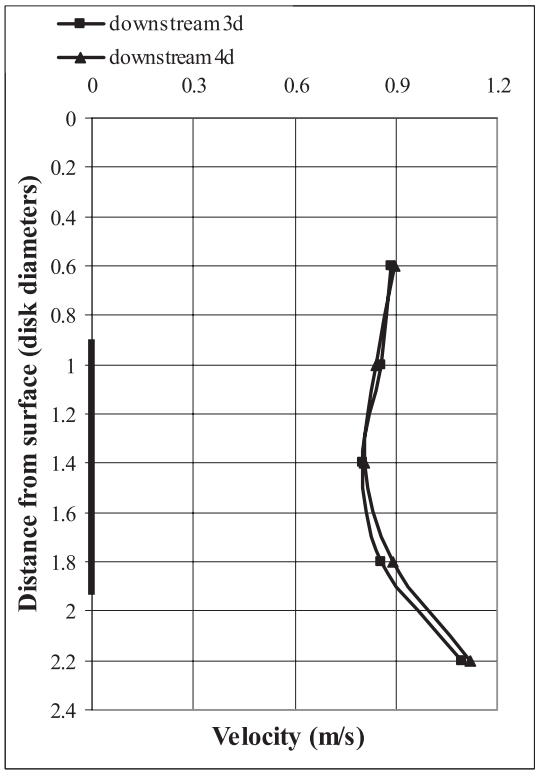

(i)

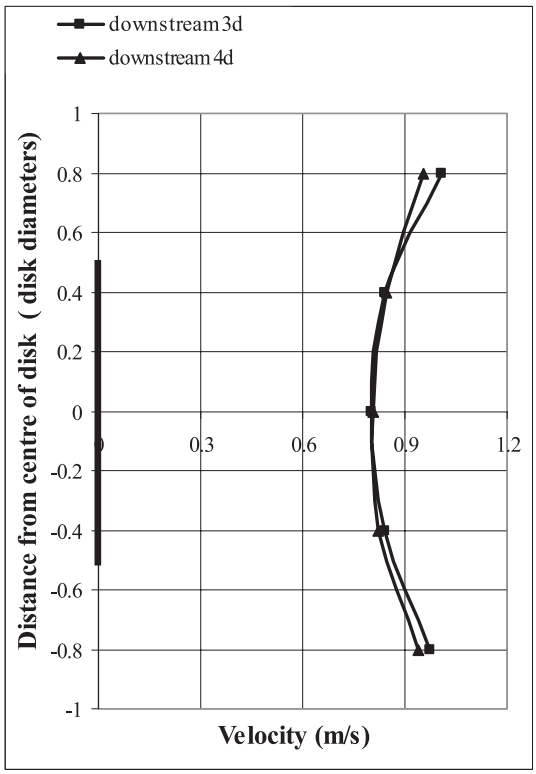

(ii)

Fig 7 (i): The initial velocity profiles in the central vertical plane at 3 and 4 diameters behind the test disk in the towing tank (the top line along the zero water depth represents the free surface)

Fig 7 (ii): The initial velocity profiles in the central horizontal plane at 3 and 4 diameters behind the test disk in the towing tank

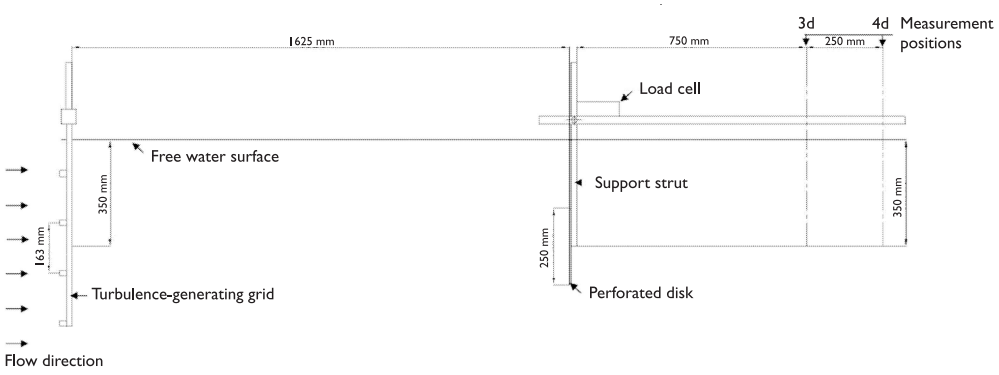

Fig 8: A schematic overview of the experimental setup in the towing tank

$$U_w = \sqrt{\frac{2\Delta p}{\rho}} \quad (2)$$

Experimental results for two perforated disks, with 14% and 50% porosity, are presented in this paper. As expected, the thrust force coefficients are approximately 1 and 0.7 respectively, which are appropriate for actual turbines typically operating at high tip speed ratios. The thrust forces measured in the towing tank are higher than that in the water flow channel, because of the higher incoming flow speed. Thrust forces and thrust force coefficients are summarised in Table 1.

In both experiments, the features of the wake are clearly observed through analysing the mean velocity profiles, which is characterised by an area of reduced velocity behind the perforated disk, which gradually recovers to the free stream velocity with downstream distance. The wake profiles resemble a Gaussian-like shape and, as the wake recovers, it loses its intensity, as shown in Figs 9 to 12. It is interesting to note that the velocity profile in the vertical plane has shown an asymmetry about the wake centerline and was especially pronounced for the results measured in the water flow channel tests. This was probably due to the

Perforated disk	T(N)	C_t
In a water flow channel, U_0= 0.76 m/s		
Disk with 14% porosity	14.11	1.00
Disk with 50% porosity	10.20	0.72
In a towing tank, U_0= 0.8 m/s		
Disk with 14% porosity	17.46	1.11
Disk with 50% porosity	11.41	0.73

Table 1: Experimental results of thrust forces and thrust force coefficients

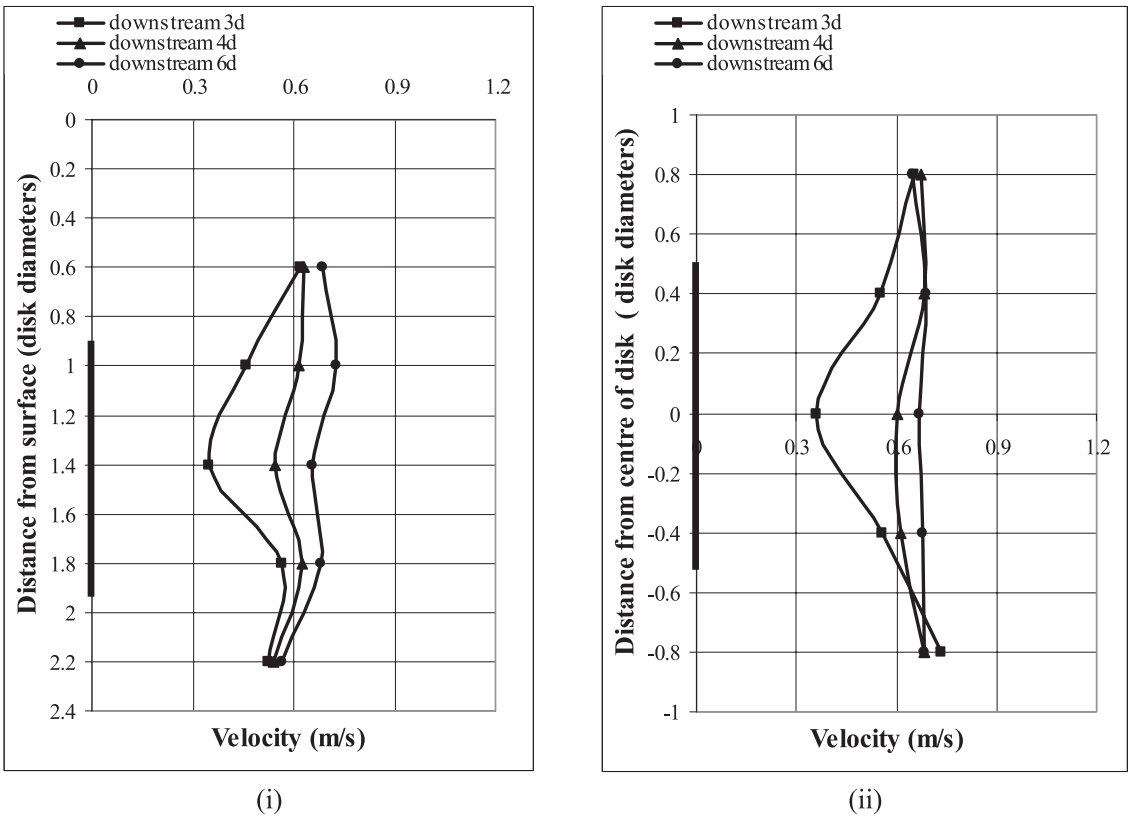

Fig 9: The wake velocity profiles in (i) the vertical plane and (ii) the horizontal plane behind a 14% porosity disk in the water flow channel

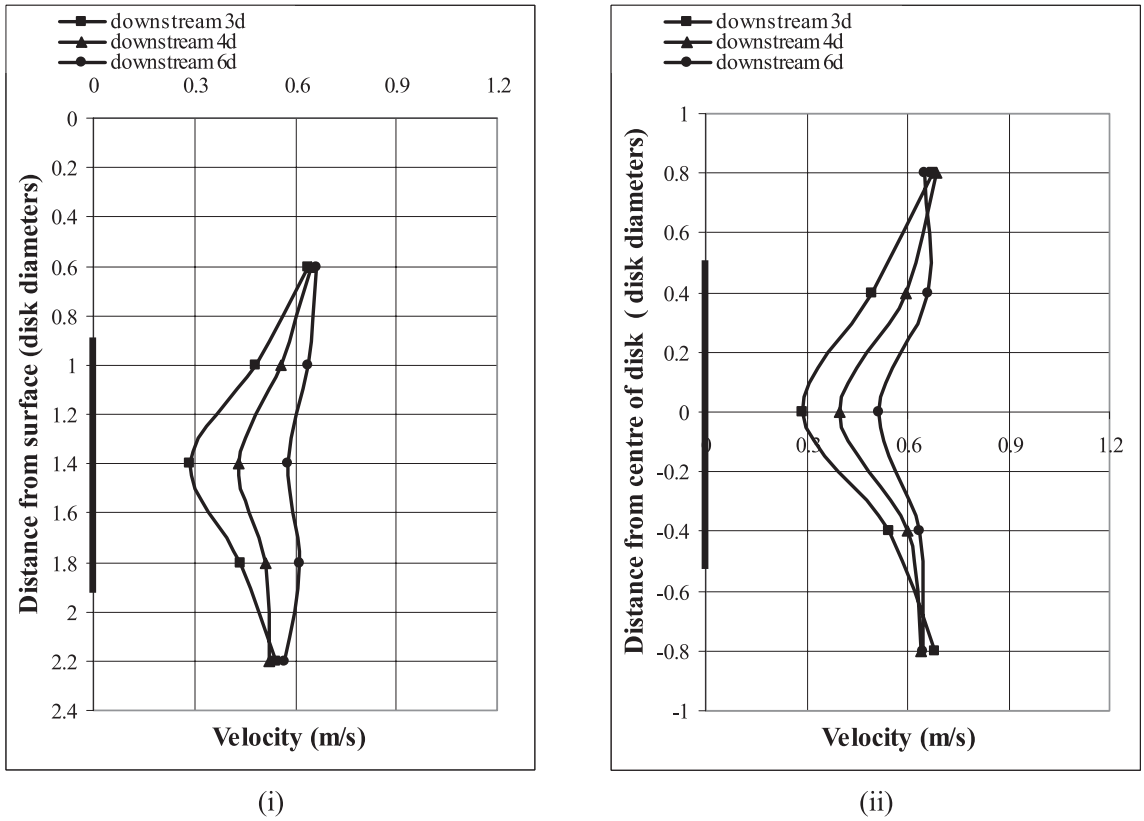

Fig 10: The wake velocity profiles in (i) the vertical plane and (ii) the horizontal plane behind a 50% porosity disk in the water flow channel

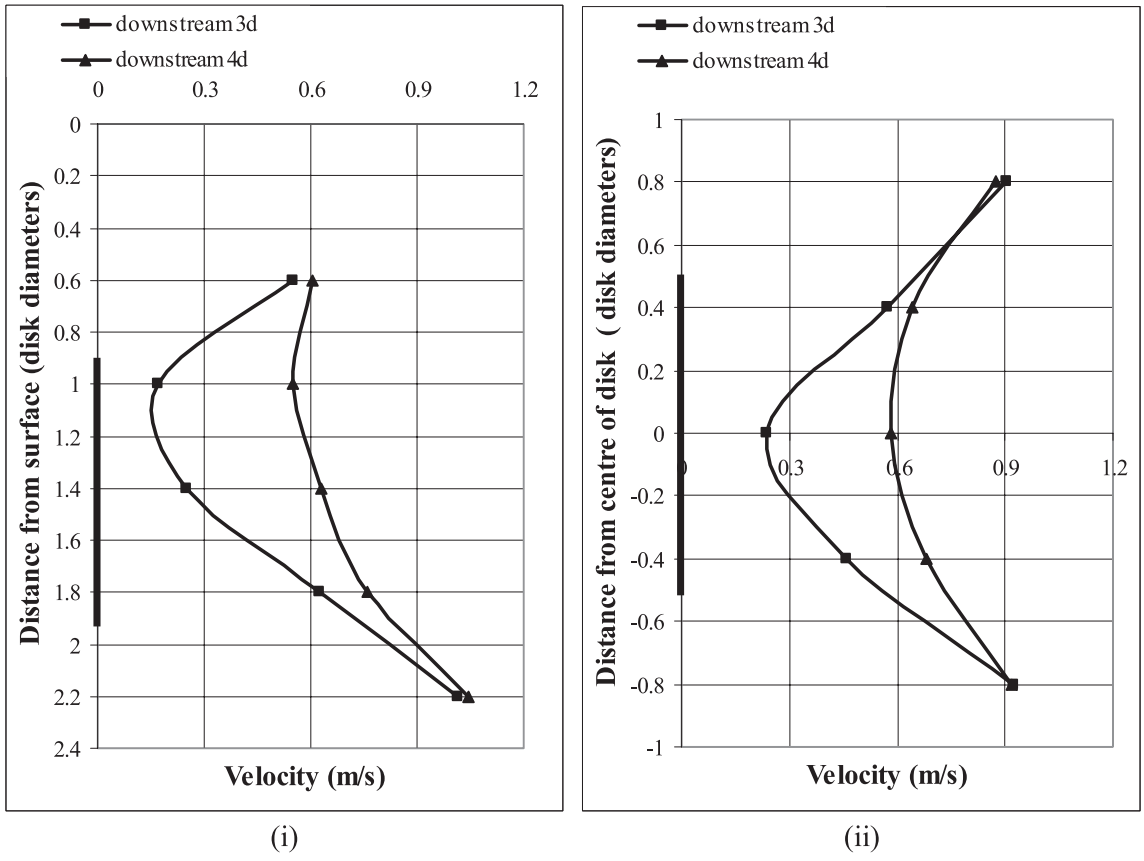

Fig 11: The wake velocity profiles in (i) the vertical plane and (ii) the horizontal plane behind a 14% porosity disk in the towing tank

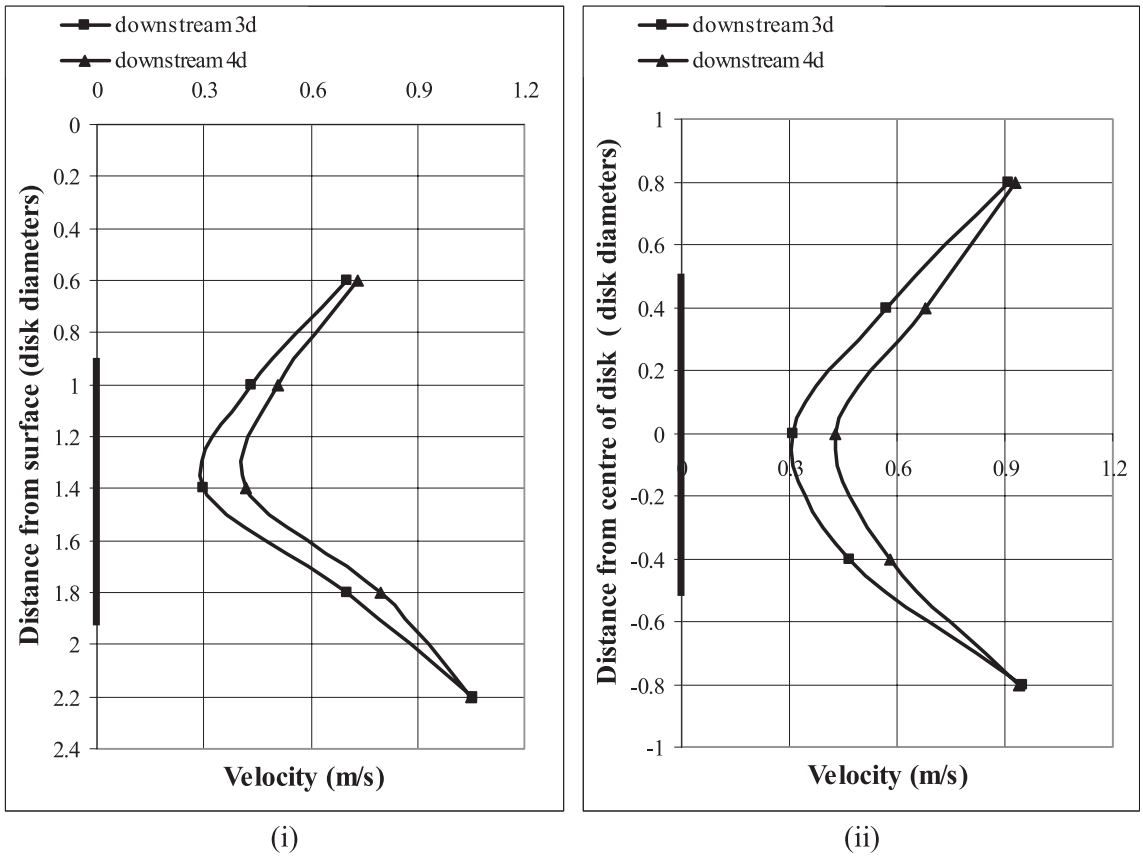

Fig 12: The wake velocity profiles in (i) the vertical plane and (ii) the horizontal plane behind a 50% porosity disk in the towing tank

influence of the aluminum strut behind the disk, but also the velocity gradient of incoming flow in the water flow channel could exaggerate this asymmetry further. The position of perforated disk in the water has been highlighted by a solid narrow black line being drawn on the left side of each figure.

Comparisons of the wake velocity deficit (the decimal percentage of initial free stream velocity) between the two experiments are made, using the wake velocity deficit in the horizontal plane, in order to reduce effects of the support strut as well as the velocity gradient in the vertical plane. The comparison results for the disk with 14% porosity are displayed in Fig 13. The profiles compare well in terms of profile shape. However, the normalised centerline velocity deficit ($=(U_0 - U_c)/U_0$), in the water flow channel tests at 3d downstream is 75%, and at 4d downstream is 73% of that in the towing tank tests. Those results are reasonable, because the much higher thrust force in the towing tank tests implies more energy loss through the disks and, therefore, results in a larger velocity deficit in the wake. For the disk with 50% porosity, the comparisons become more favourably because of the similar thrust forces obtained and the distribution of the forms of the wake profiles shows the closest agreement with each other, as presented in Fig 14. Less symmetric in-flow conditions cause less symmetric wake profiles in the water flow channel and are the reason for the discrepancy in the lower part of the profiles.

CONCLUSIONS

An experimental survey in the wake of tidal current turbine has been carried out. Perforated disks were used to simulate turbines, although there do exist some differences. For instance, the rotation of a turbine wake due to the rotating turbine blades is neglected and the vortices shed from the edge of the turbine are different from those of the disk. However, the vortices can decay quickly within a short downstream distance and these factors are not considered the most critical features in the downstream wake re-energisation process,[12] which has the most interest for a tidal 'farm'. Measurements were conducted at known distances behind the disk.

The experimental results have helped identify the generic features of horizontal axis tidal current turbine wakes, on which little work has been done. Two different flow conditions were applied. Field tests in a water flow channel replicated the actual operating condition for tidal current turbines. However, the elaborate measuring equipment was difficult to apply in field conditions and the lack of control directly limited the important parameters, which are related to the wake development like flow speed and ambient turbulence, to be investigated. A traditional towing tank has been confirmed as suitable for the preliminary model testing of tidal current turbines, since the same thrust force coefficient and similar downstream wake profiles as those measured in a water flow channel are obtained. The towing tank has, in addition, the advantage of controllable and

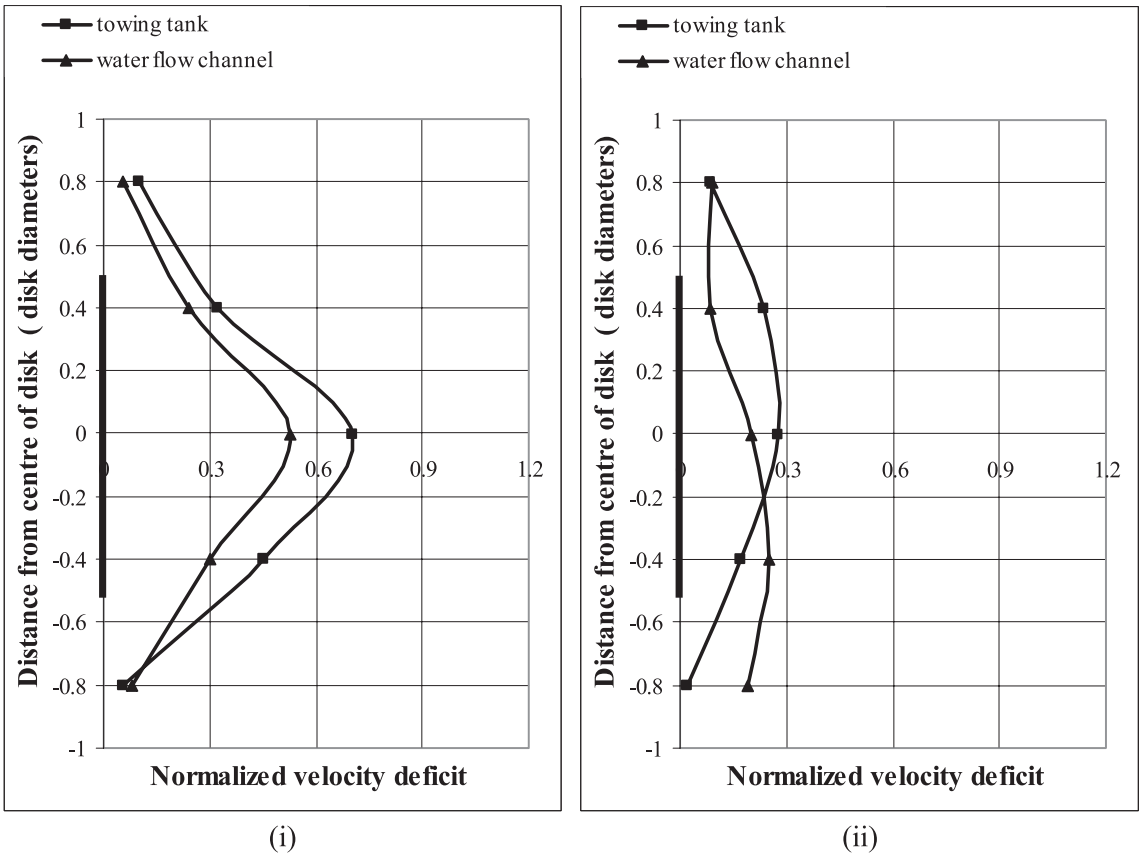

(i) (ii)

Fig 13: Comparison of wake deficit profiles for the 14% porosity disk at (i) downstream 3*d* and (ii) downstream 4*d* in the water flow channel and the towing tank

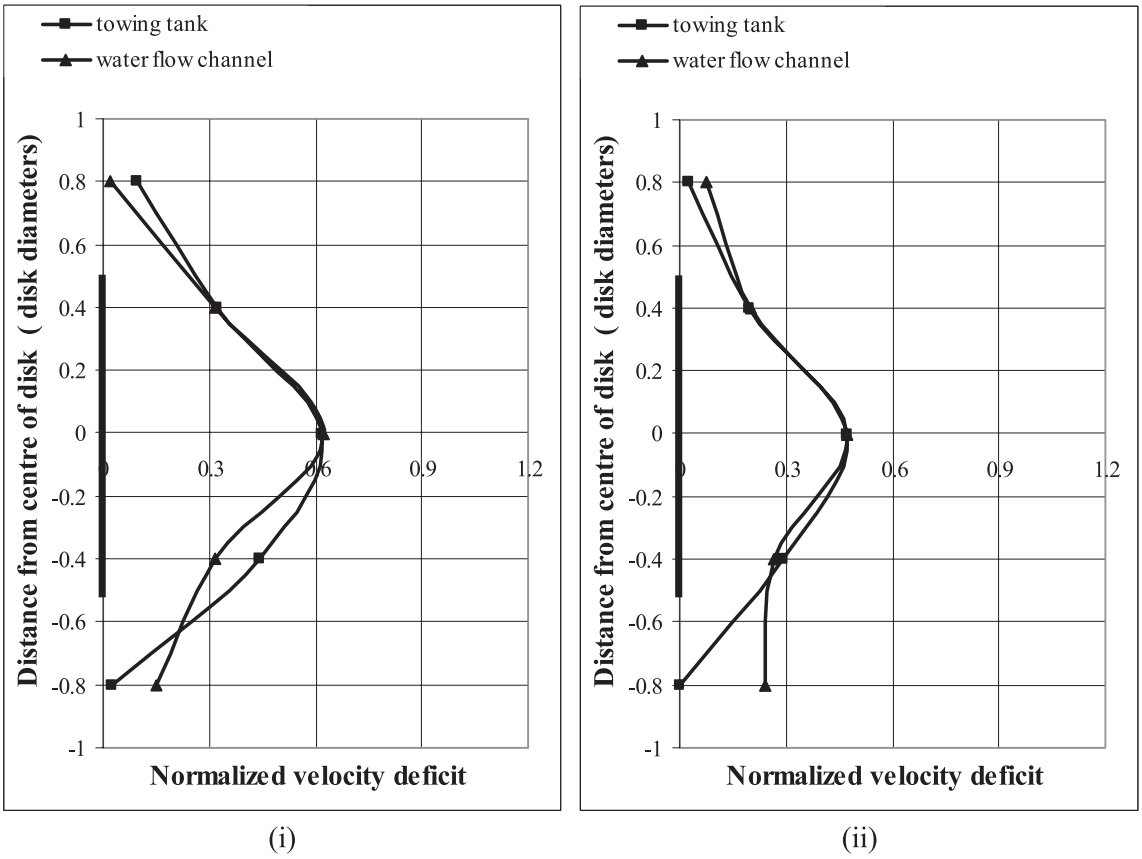

(i) (ii)

Fig 14: Comparison of wake deficit profiles for the 50% porosity disk at (i) downstream 3*d* and (ii) downstream 4*d* in the water flow channel and the towing tank

repetitive laboratory conditions. Hence a large towing tank can allow tidal current devices to be tested at different scales over a wide range of water speeds. Therefore, a towing tank is particularly useful at a time when experimental facilities specifically designed to study the tidal current energy devices are still under development.

ACKNOWLEDGEMENT

The authors wish to thank the Engineering and Physical Science Research Council (EPSRC) for their support of the Supergen (marine) consortium, which has funded much of this work and Scottish and Southern Energy PLC (SSE) for arranging access for SuperGen (marine) to the moving water test site at Quoich Power Station near Invergarry. The Acre Road Hydrodynamics Laboratory of the Universities of Glasgow and Strathclyde is gratefully acknowledged for providing the towing tank and assistance during the tank test. The Edinburgh based authors also acknowledge the support of the Scottish Funding Council for the Joint Research Institute with the Heriot-Watt University which is a part of the Edinburgh Research Partnership.

REFERENCES

1. ETSU, Tidal stream energy review. 1993. UK DTI. Prepared by Engineering & Power Development Consultants Ltd, Binnie & Partners, Sir Robt. McAlpine & Sons and IT Power Ltd, for the ETSU, UK Department of Energy. Report No. ETSUT/05/00155/REP, Crown Copyright, 1993.

2. Black & Veatch. Europe and global tidal stream energy resource assessment. Report to Carbon Trust, 2004.

3. FREDS(MEG), Harnessing Scotland's Marine Energy Potential. Published by the Scottish Executive, 2004.

4. SDC, Turing the tide, tidal power in the UK. 2007. Available online: http://www.sd-commission.org.uk/publications.php?id=607

5. Kostas Rados. 2003. Optimisation of tidal farms. EPSRC individual grant review report-GR/N04805/01.

6. Bryden IG, Grinsted T and Melville GT. 2005. *Assessing the potential of a simple tidal channel to deliver useful energy.* Applied Ocean Research, Vol. 26, pp 200-206.

7. Bahaj AS, Myers LE, Thomson MD and Jorge N. 2005. *Characterising the wake of horizontal axis marine current turbines*. In: Proceedings of the seventh EWTEC European wave and tidal energy conference.

8. Medici D and Alfredsson PH. 2006. *Measurements on a wind turbine wake: 3D effects and bluff body vortex shedding.* Wind Energy, Vol 9, pp219-236.

9. Wentz W, Ostowari C, Manor D and Snyder M. 1985. *Horizontal axis wind turbine wake and blade flow studies from model tests.* ASME, pp235-244.

10. Sforza PM, Sheerin P and Smorto M. 1981. *Three-dimensional wakes of simulated wind turbines*. AIAA Journal, Vol 19, pp1101-1107.

11. Lissaman PBS. 1979. *Energy effectiveness of arbitrary arrays of wind turbines.* AIAA paper, 17th Aerospace Sciences Meeting.

12. Medici D and Alfredsson PH. 2005. *Wind turbine near wakes and comparisons to the wake behind a disc.* 43rd AIAA Aerospace Sciences Meeting and Exhibit-Meeting Papers, pp15593-15604.